Applied Magnetic Resonance (2020) 51:993–1003
https://doi.org/10.1007/s00723-020-01250-w

Applied
Magnetic Resonance

ORIGINAL PAPER

Integral Intensity of the EPR Signal of NO Molecules Adsorbed on Lewis Acid Sites of Oxide Systems as a Function of Surface Coverage

Aleksandr A. Shubin[1,2] · **Alexander M. Volodin**[1]

Received: 19 July 2020 / Revised: 5 August 2020 / Published online: 21 September 2020

Abstract
A simple model is proposed that semi-quantitatively explains the dependence of the EPR signal intensity of adsorbed NO molecules on the adsorption value. It is assumed that there are only two types of NO adsorption sites on each facet of the microcrystal, such that only NO molecules adsorbed on one of them are active in EPR. Within the framework of this model of lattice adsorption, it is assumed that there are Z other adsorption centers from the set under consideration that are available for the adsorption of neighboring NO molecules in the local environment of each EPR-active adsorption center. In this case, the formation of diamagnetic $(NO)_2$ dimers containing an NO molecule adsorbed on a center active in the EPR decreases the integral intensity of the EPR signal. Analytical expressions are obtained for the dependence of the EPR signal intensity on the surface coverage. They were used to analyze experimental data on the adsorption of NO at the Lewis acid sites of sulfated zirconia. The proposed model consistently explains the results of EPR experiments.

1 Introduction

The 15-electron molecule of nitric oxide (NO) has a ground electronic state $^2\Pi_r$, in which the $^2\Pi_{3/2}$ sublevel is located about 122 cm^{-1} above the lowest $^2\Pi_{1/2}$ sublevel. The latter of them has a vanishingly small magnetic moment, while the $^2\Pi_{3/2}$ sublevel has an extremely anisotropic g-tensor ($g_{\parallel} - g_{\perp} \approx 4$). As a result, the observation of the EPR spectrum for *matrix-isolated randomly oriented* NO molecules is practically impossible at any temperatures. At low temperatures, the $^2\Pi_{3/2}$ sublevel is not populated, and at higher temperatures the spectrum is diffi-

✉ Aleksandr A. Shubin
a.a.shubin@catalysis.ru

[1] Boreskov Institute of Catalysis, Pr. Lavrentieva, 5, Novosibirsk 630090, Russia

[2] Novosibirsk State University, 1, Pirogova str., Novosibirsk 630090, Russia

cult to detect due to the extremely large width of the EPR signal. In the case of NO adsorption on strong surface centers, the degeneracy in $^2\Pi_r$ can be lifted due to the interaction with coordinatively unsaturated ions existing on surface. This makes it possible to observe the EPR spectra of paramagnetic NO molecules in the adsorbed state, the EPR parameters of these molecules depend on the magnitude of the splitting of π-orbitals in the crystal field of the stabilizing cation [1–3].

The NO molecule possesses donor properties and, upon adsorption, stabilizes primarily at the electron-acceptor Lewis acid sites (LAS) of the surface of oxide systems:

$$\mathrm{NO} + \mathrm{LAS} \Leftrightarrow [\mathrm{NO} \ldots \mathrm{LAS}]. \quad (1)$$

For this reason, it is often used as a spin probe for studying Lewis acid sites on the surface of zeolite catalysts, as well as other oxide systems with various types of coordinatively unsaturated structures [1–12]. Another possibility of using this molecule as a paramagnetic probe is the formation of nitrosyl complexes with half-integer spin when interacting with integer-spin metal ions stabilized on the surface of oxide catalysts [13–15]:

$$\mathrm{Me}^{n+} + \mathrm{NO} \Leftrightarrow \left[\mathrm{Me}^{n+} \ldots \mathrm{NO}\right]. \quad (2)$$

Correct determination of the concentration of adsorption centers in such experiments is complicated by the tendency towards the formation of diamagnetic $(NO)_2$ dimers during adsorption. This leads to a nonlinear dependence of the concentration of the formed paramagnetic complexes on the concentration of adsorbed NO molecules. This effect is known in the literature and was observed in the study of active centers on the surface of various types of oxide systems [4, 11, 12, 16]. It is quite natural to assume that the number of paramagnetic complexes detected by the EPR method will reflect the real concentration of the studied active centers and will linearly depend on the concentration of adsorbed NO molecules only at a sufficiently low surface coverage of these molecules and only if the heat of formation of complexes [NO…LAS] higher than the heat of physical adsorption of NO on the rest of the surface and higher than the heat of formation of diamagnetic dimers $(NO)_2$. With an increase in the concentration of adsorbed NO molecules, it becomes possible the stabilization of NO molecule near the already existing paramagnetic complex [NO…LAS], accompanied by the loss of paramagnetism due to the formation of a diamagnetic dimeric structure. In this regard, the purpose of this work is to analyze the effect of surface coverage with NO molecules on the number of paramagnetic complexes [NO…LAS] detected by the EPR method within the framework of the lattice model assuming the presence of Z centers of adsorption available for NO molecules in the first coordination sphere of [NO…LAS]. It is assumed that the appearance of such molecules leads to the formation of diamagnetic dimers and the disappearance of the EPR spectra of the [NO…LAS] complexes. A sample of sulfated ZrO_2, which we studied earlier and for which the influence of the amount of adsorbed NO on the concentration of the observed paramagnetic complexes [NO…LAS] was revealed, was chosen as the object of investigation [16].

2 Methods

Sulfated zirconia was used, its synthesis is described in [16]. A sample with a specific surface area $S = 130$ m^2 g^{-1} contained 4.6 wt% SO_3. EPR spectra were recorded in situ using the setup described in detail in [17]. 0.1 g of the catalyst was placed in a quartz ampoule connected to a high-vacuum system. Before performing EPR measurements in situ, the sample was preliminarily treated in an oxygen atmosphere (10 Torr) at 773 K with freezing of the obtained products in a trap cooled with liquid nitrogen. The purpose of this treatment is to dehydrate the sample surface and remove biographic organic contaminants from it. This was followed by cooling the sample in an oxygen atmosphere and evacuation for 30 min at room temperature. NO adsorption was carried out at 143 K; the amount of adsorbed NO and its presence in the gas phase were monitored manometrically. After the experiment, the original state of the sample was regenerated in accordance with the above procedure.

3 Results and Discussion

Typical EPR spectra appearing upon the adsorption of various amounts of NO molecules on the sample under study at $T = 143$ K are shown in Fig. 1. At this temperature, it is quite easy to reversibly vary the amount of adsorbed NO molecules on the surface of the sample, changing the pressure of the gas phase and thereby shifting the adsorption equilibrium:

$$\text{Surf} + \text{NO} \Leftrightarrow \text{NO}_{\text{ads}}. \tag{3}$$

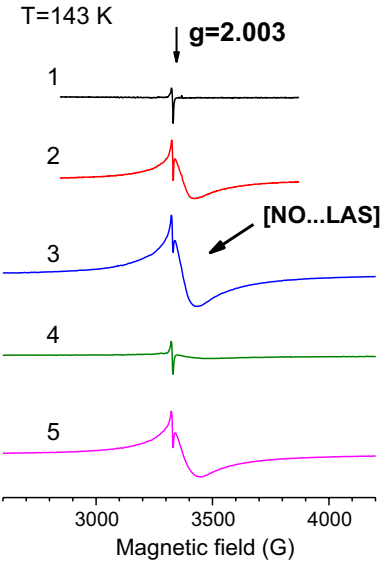

Fig. 1 EPR spectra of the initial sample before (spectrum 1) and after adsorption of NO molecules in an amount of 1.6×10^{19} [1.2%] (spectrum 2); 3×10^{20} [23%] (spectrum 3); and 5×10^{20} [38%] (spectrum 4) molecules g^{-1} [% monolayer], as well as after additional short-term evacuation of the sample at 143 K (spectrum 5)

Naturally, under such conditions, NO adsorption can occur both in the form of paramagnetic complexes of the [NO…LAS] type upon adsorption on LAS, and in the form of diamagnetic $(NO)_2$ dimers upon physical adsorption on the rest of the sample surface. It should be noted that the heat of adsorption of NO molecules on LAS is much higher than the heat of their physical adsorption. For this reason, short-term evacuation at 143 K leads, first of all, to the removal of physically adsorbed NO molecules while maintaining a constant concentration of paramagnetic complexes of the [NO…LAS] type. We also note that at a temperature of 143 K, a rather wide and unresolved EPR spectrum of the [NO…LAS] complexes with an average value of $g_{av} = 1.98$ is observed, which is typical for them in this system [16]. The significant width of the observed signal is due to the dynamics of the motion of NO molecules on the catalyst surface at this temperature. The narrow signal in the g_e region (Fig. 1, spectrum 1) is due to the presence of bulk defects in the initial sample; it does not change upon adsorption of NO and is not discussed further. It is important to note that the shape of the signal from paramagnetic [NO…LAS] complexes does not depend on the concentration of adsorbed NO molecules and is the same for all those shown in Fig. 1 spectra. It is significant that it does not change at high concentrations of adsorbed NO molecules (Fig. 1, spectrum 4), when a strong fall of the concentration of paramagnetic complexes detected by the EPR method is observed. This means that no noticeable effect of signal broadening due to dipole–dipole interactions with adsorbed NO molecules on the EPR signal intensity measured under the conditions of our experiments is observed. It is quite logical to assume that the observed effect is associated with the disappearance of the paramagnetism of the [NO…LAS] complex, due to the formation of a diamagnetic dimer of the $[(NO)_2$…LAS] type, when another paramagnetic NO molecule appears next to this [NO…LAS] complex. Also note that the removal of excess adsorbed NO by short-term evacuation practically restores the maximum concentration of paramagnetic [NO…LAS] complexes detected by the EPR method (Fig. 1, spectrum 5). This indicates the reversibility of the processes of adsorption–desorption of NO in our experiments and the invariable state of the surface centers of the catalyst. At the same time, the possibility of "disappearance" of the EPR spectra from paramagnetic complexes [NO…LAS] due to the formation of diamagnetic dimers significantly complicates the quantitative assessment of the concentration of the LAS under study in such experiments.

The dependence of the concentration of paramagnetic complexes [NO…LAS], detected by the EPR method, on the surface coverage by adsorbed NO molecules is shown in Fig. 2.

As can be seen, with a specific surface area of 130 $m^2\ g^{-1}$, the maximum number of spins is observed in EPR with a surface coverage of $\theta = 0.069$, which corresponds to $9.0 \times 10^{19}\ g^{-1}$ adsorbed NO molecules. As noted in the Sect. 1, the subsequent drop in the signal with increasing θ is due to the formation of diamagnetic dimers of the $[(NO)_2$…LAS] type. Our goal was to characterize the distribution of strong NO adsorption sites in the catalyst based on the experimental data presented in Fig. 2. Note that the catalyst surface is actually a collection of different facets of chaotically oriented microcrystals. To describe the adsorption of NO on the particular facet

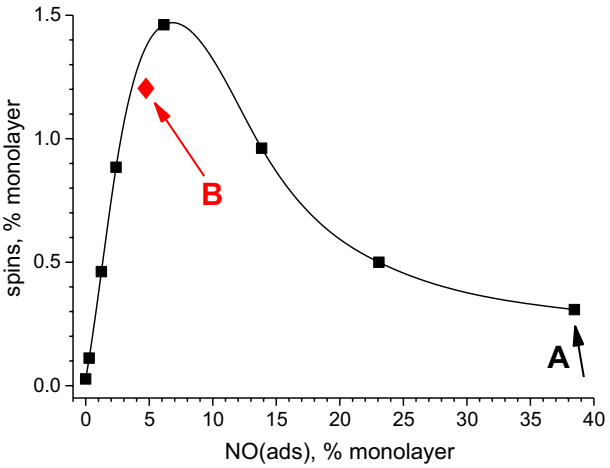

Fig. 2 Dependence of the number of [NO…LAS] complexes detected by the EPR method on the surface coverage by adsorbed NO molecules at 143 K. Point A corresponds to the maximum filling of the surface with adsorbed NO molecules. Point B—after additional short-term evacuation of the gas phase above the sample at 143 K

of the microcrystal, we used the simplest two-site Langmuir isotherm model with quite distant Henry's law constants of the two sites, thereby neglecting the small, but experimentally measurable, energy of lateral interaction between neighboring NO molecules. To apply this isotherm to the description of EPR experiments, the following assumptions were used. (a) Only NO molecules adsorbed on strong centers [NO…LAS] can be observed in EPR; (b) regardless of the strength of the center, the NO molecule on it is inactive in EPR if at least one of the Z neighboring centers is occupied by another NO molecule; (c) any of the Z neighbors of the strong (LAS) site with the α probability is the LAS, and with the $1 - \alpha$ probability—the weak adsorption site, where α is the fraction of LAS for a given facet of the microcrystal. Based on this model, it is possible to analytically determine the intensity of the EPR signal as a function of the degree of surface coverage of the considered type of microcrystal facets. A more detailed derivation of the mathematical relationships of the model is given in the "Appendix".

Comparison of the curve in Fig. 2 with the model dependencies shown in Figs. 5 and 6, shows that the noticeable value of the EPR signal in Fig. 2 at $\theta \approx 0.4$ is difficult to explain with this model. This is not surprising, since the total specific surface of the sample is a combination of the most different types of microcrystal facets. As further consideration shows, quite satisfactory agreement with experiment can be obtained when considering, under the conditions of this model, the adsorption of NO only on two substantially different types of crystal facets (see Fig. 3).

Crystalline facets of the first type contain only strong LAS and weak adsorption centers, while facets of the second type mainly contain superweak centers of physical adsorption and isolated LAS. It is the adsorption on the latter that corresponds to the tail of the experimental curve in Fig. 2 at $\theta \approx 0.4$, since in this case most of the centers of superweak physical adsorption are not yet occupied by NO molecules. For

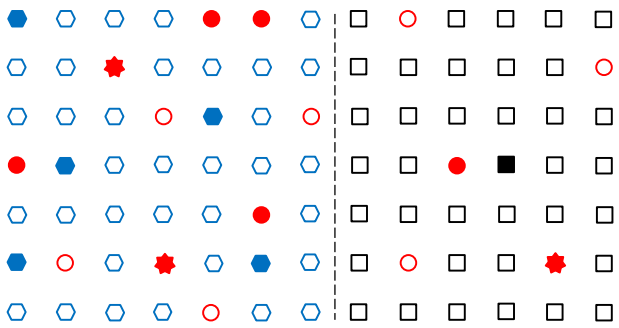

Fig. 3 The model of the surface used to interpret the experimental data presented in Fig. 2. On the left, the figure shows the facet of microcrystallite; this facet contains only strong (red) and weak (blue hexagons) NO adsorption sites. The right side of the figure shows the facet of microcrystallite, which contains only rare strong (red) adsorption centers, surrounded by superweak centers (black squares) of physical adsorption of NO. Solid fill indicates the centers where adsorbed NO molecules are already present, including (7-pointed red stars) strong centers that contribute to the EPR signal (color figure online)

this reason, they do not form diamagnetic dimers with the NO molecule, which is part of the [NO…LAS] paramagnetic complex.

To approximate and then exclude from consideration the adsorption of NO on the facets of the second type, the following procedure was proposed. We assume that the adsorption energy of NO on LAS is approximately the same for facets of all types, also assume that almost all LAS at $\theta > 0.07$ are already occupied by NO molecules, since the adsorption of NO on the facets of the first type is still predominantly continuing. Therefore, at $0.07 < \theta \leq 0.4$ in the first approximation, the adsorption of NO on the facets of the second type is mainly determined by the adsorption on the LAS of these facets (constant value given by the last point in Figs. 2 or 4a). Further, at

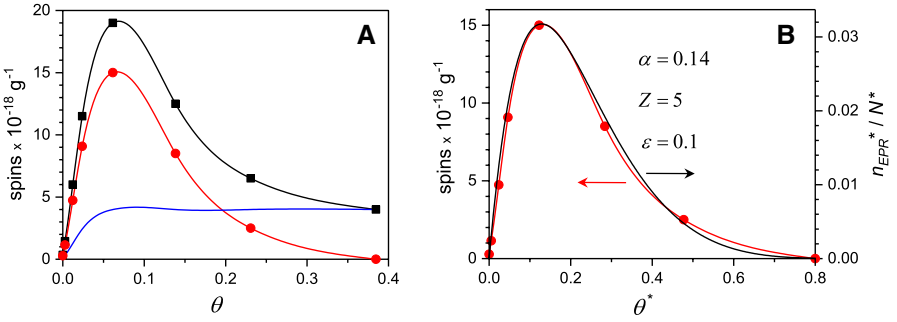

Fig. 4 **a** Possible decomposition of the experimentally observed dependence of the EPR signal intensity (here, black line and squares), previously shown in Fig. 2 into two components. The first of them (red line and circles) is the contribution of NO molecules located on strong adsorption centers of the facets of the first type of sulfated zirconia microcrystallites (see the left side of Fig. 3), and the second contribution (in blue) corresponds to NO molecules adsorbed on rare strong centers of microcrystallite facets with a predominant content of centers of weak physical adsorption (see the right side of Fig. 3). **b** Modeling of the first contribution using a relation similar to Eq. (9); the rest of the explanation is given in the text (color figure online)

$0 \le \theta \le 0.07$, we approximate the adsorption at the LAS of the facets of the second type by the corresponding segment of the curve from Fig. 2 times the scaling factor (compare with Fig. 6a, which shows the results of calculations for adsorption centers that differ significantly in strength). Subtracting from the total number of centers observed in EPR the contribution from adsorption on LAS centers of facets of the second type (blue curve in Fig. 4a), we obtain the EPR intensity of NO molecules located on the facets of the first type (red curve in Fig. 4a).

The last, perhaps the most controversial issue, is the relationship between the surface coverage θ^* for the facets of the first type and the experimentally measured integral surface coverage θ. Numerous test calculations using relation Eq. (9) show that with a reasonable choice of the ratio $\varepsilon = K_1/K_2$ of equilibrium constants and other parameters, the last point on the experimental curve (Fig. 4a) should correspond to $\theta^* \approx 0.7$–0.9 (see, for example, Fig. 5b). Figure 4b shows (in red) the experimental dependence of the EPR signal intensity n^*_{EPR} of NO molecules adsorbed on the facets of the first type, already scaled to $\theta^* = 0.8$. The relation Eq. (9) was used in the form $n^*_{\mathrm{EPR}} = N^*\theta^*_1(1-\theta^*)^Z$, where N^* is the total number of adsorption sites (g^{-1}) of the LAS type and centers of weak adsorption on the facets of the first type in the sample under study. Ibid, in Fig. 4b, the black curve shows the theoretical relationship corresponding to the following choice of parameters: $\varepsilon = \frac{K_2}{K_1} = 0.1$; $Z = 5$—the number of neighbors for each LAS center; $\alpha = 0.14$—relative portion of LAS on facets of the first type. Based on the maximum of the experimental curve $n^*_{\mathrm{EPR}} = 1.5 \times 10^{19}\ g^{-1}$ and the theoretically found maximum $\frac{n^*_{\mathrm{EPR}}}{N^*} = 0.032$, it can be estimated that there are about $3.1 \times 10^{20}\ g^{-1}$ adsorption sites for NO molecules on the facets of the first type, which is a quarter of the total $1.3 \times 10^{21}\ g^{-1}$ number of adsorption sites. Now, taking into account the obtained value, we estimate that the actual number of LAS on the facets of the first type is approximately 3.5% of the monolayer (the total number of adsorption sites on all facets). It is clear that due to the very simple surface model that we used due to the limited set of experimental data, the obtained $Z = 5$ is only some effective value. However, we note that for the basal crystal facets of the tetragonal phase of zirconia, one should expect $Z \sim 4$, which is close to the experimentally found value.

4 Conclusion

The NO molecule is often used as a spin probe to detect Lewis acid sites on the surface of various oxide catalysts. With its help, the presence of such centers is reliably detected and information is obtained on the effective charge of the cations included in them. At the same time, obtaining data on the real concentration of such centers is a rather difficult task. This is due to the fact that the NO molecule is not only stabilized on the LAS with the formation of paramagnetic complexes detected by the EPR method, but also with its stabilization on other surface centers in the form of diamagnetic dimers. With an increase in the concentration of adsorbed NO molecules, such a dimerization process can also include NO molecules stabilized on the

LAS, which leads to a decrease in the concentration of the detected paramagnetic complexes. In this work, we propose a lattice model that assumes a statistical distribution of the detected LAS and other centers of NO adsorption on the catalyst surface, which makes it possible to take into account the effect of a decrease in the concentration of the detected paramagnetic complexes [NO…LAS] with an increase in the concentration of adsorbed molecules. The proposed model semi-quantitatively describes the experimental data for sulfated zirconia and makes it possible to estimate the real concentration of LAS present in the sample (~3.5% monolayer), which is more than 2 times higher than the maximum observed in the EPR experiment. Along with this, it turns out to be possible to reveal the presence of areas on the surface of the test sample, which differ significantly in the local concentration of LAS and other centers of NO adsorption.

The approach proposed in this work can be used to obtain information on the actual amount of LAS in various catalysts using the NO molecule as a spin probe.

Acknowledgements The authors are grateful to Dr. D. K. Efremov for the sincere interest shown in this work.

Appendix

EPR Signal Intensity of Adsorbed NO Molecules as a Function of Surface Coverage in the Framework of the Two-Site Langmuir Isotherm Model

The experimentally observed dependence of the EPR signal intensity on the surface coverage can be qualitatively, and even semi-quantitatively, explained already within the framework of the simplest two-site model of localized Langmuir monomolecular

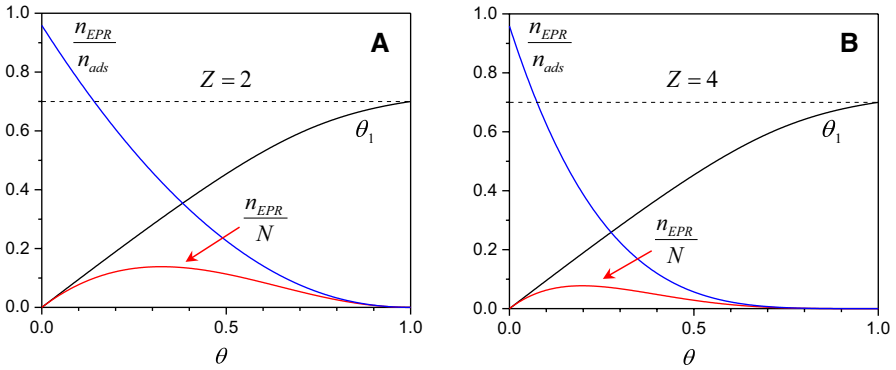

Fig. 5 Dependence of the contribution (θ_1) of NO adsorption on strong adsorption centers to the total surface coverage θ at a relative fraction of strong centers $\alpha = 0.7$ and a ratio of equilibrium constants for weak and strong centers $\varepsilon = 0.1$. Also for cases $Z = 2$ (**a**) and $Z = 4$ (**b**), the EPR signal intensities of adsorbed NO molecules normalized to the total number of surface adsorption centers $\frac{n_{EPR}}{N}$ and normalized to the current total number of adsorbed NO molecules $\frac{n_{EPR}}{n_{ads}}$ are shown

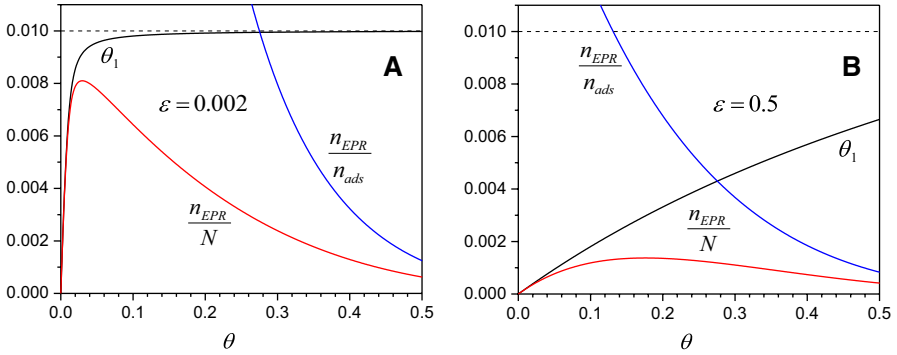

Fig. 6 Dependence of the contribution (θ_1) of NO adsorption on strong adsorption centers to the total surface coverage θ at a relative fraction of strong centers $\alpha = 0.01$ and $Z = 4$. The designations are the same as in Fig. 5; $\varepsilon = 0.002$ (**a**) and $\varepsilon = 0.5$ (**b**)

adsorption [18–22]. Hereinafter, we will adhere to the notation used in [19]. For this model of monomolecular adsorption, the following expression is valid for the surface coverage θ:

$$\theta = \theta_1 + \theta_2 = \frac{\alpha K_1 C}{1 + K_1 C} + \frac{(1-\alpha) K_2 C}{1 + K_2 C}. \tag{4}$$

Here, $0 < \alpha \leq 1$ is the relative fraction of strong adsorption centers (that is, NO molecules adsorbed on them give an easily observed EPR signal). $\theta_1 = n_1/N$ and $\theta_2 = n_2/N$ are contributions to θ due to the fact that n_1 NO molecules are adsorbed in equilibrium on the strong, and n_2 NO molecules are adsorbed on the weak centers, respectively. $N = N_1 + N_2 = \alpha N + (1-\alpha)N$ is the total number of adsorption sites, N_1 of which are strong and N_2 are weak. K_1 and K_2 are the Langmuir adsorption equilibrium constants for sites 1 and 2, respectively. C is the concentration of NO (equilibrium adsorption pressure).

Let's define the ε parameter as $\varepsilon = K_2/K_1$, then the expression for θ_2 can be rewritten as:

$$\theta_2 = \frac{(1-\alpha) K_2 C}{1 + K_2 C} = \frac{\varepsilon(1-\alpha)\theta_1}{\alpha - (1-\varepsilon)\theta_1}. \tag{5}$$

Further, substituting Eqs. (5) in (4), we obtain a quadratic equation with respect to θ_1, the solution of which, satisfying the conditions $\theta_1(\theta = 0) = 0$ and $\theta_1(\theta = 1) = \alpha$, has the form:

$$\theta_1 = \frac{\alpha + \theta}{2} + \frac{\varepsilon - \sqrt{[\theta - \alpha + \varepsilon(1-\alpha-\theta)]^2 + 4\varepsilon\alpha(1-\alpha)}}{2(1-\varepsilon)}. \tag{6}$$

For $\theta \ll 1$, the following expansion of Eq. (6) in powers of θ is valid:

$$\theta_1 \approx \frac{\alpha}{\alpha + \varepsilon(1-\alpha)}\theta - \frac{\varepsilon(1-\varepsilon)\alpha(1-\alpha)}{(\alpha+\varepsilon(1-\alpha))^3}\theta^2. \tag{7}$$

It makes sense to give here other useful, but not used in this article, consequences of relation Eq. (6):

$$\begin{aligned} \theta_1 &\approx \theta\left(1 - \frac{\varepsilon(1-\alpha)}{\alpha-\theta}\right) \quad \text{if} \quad 0 \le \theta < \alpha \quad \text{and} \quad \varepsilon \ll \alpha - \theta \\ \theta_1 &\approx \alpha\left(1 - \frac{\varepsilon(1-\theta)}{\theta-\alpha}\right) \quad \text{if} \quad \alpha < \theta \le 1 \quad \text{and} \quad \varepsilon \ll \theta - \alpha. \end{aligned} \tag{8}$$

At this stage, let's formalize our model for the EPR signal intensity of adsorbed NO molecules, namely: (a) NO molecules adsorbed on weak centers are not experimentally observed due to the strong broadening of the EPR signal; (b) NO molecules adsorbed on strong adsorption centers are observed in the EPR only if all centers adjacent to them (regardless of their strength) are free of NO molecules; (c) each of the strong adsorption centers has Z neighboring centers, and each of the neighbors with probability α is a strong adsorption center and, accordingly, with a probability of $1-\alpha$—weak. In these approximations, the number of NO molecules n_{EPR} contributing to the EPR signal becomes less than $n_1 = \theta_1 N$ and is determined by the formula:

$$n_{\mathrm{EPR}} = n_1(1-\theta)^Z = N\theta_1(1-\theta)^Z. \tag{9}$$

Here $(1-\theta)$ is the probability that the given adsorption site, adjacent to the strong center under consideration, is free of the NO molecule. Indeed, according to condition (c) formulated above, the probability w that this neighboring site contains the NO molecule is $w = \alpha\frac{n_1}{N_1} + (1-\alpha)\frac{n_2}{N_2} = \theta_1 + \theta_2 = \theta$. From (9) we get the main relation of our model:

$$\frac{n_{\mathrm{EPR}}}{n_{\mathrm{ads}}} = \frac{\theta_1}{\theta}(1-\theta)^Z, \tag{10}$$

where $n_{\mathrm{ads}} = \theta N = n_1 + n_2$ is the total number of adsorbed NO molecules, and θ_1 is determined by the formula (6). Two examples of numerical calculations performed using formulas (6) and (9) are shown in Fig. 5.

Note that using decomposition Eq. (7), two *exact* relations that can be useful in analyzing the experimental dependence of n_{EPR} on θ can be obtained:

$$\lim_{\theta\to 0}\left(\frac{n_{\mathrm{EPR}}}{n_{\mathrm{ads}}}\right) = \frac{\alpha}{\alpha+\varepsilon(1-\alpha)} \tag{11}$$

$$\frac{d}{d\theta}\left(\frac{n_{\mathrm{EPR}}}{n_{\mathrm{ads}}}\right)_{\theta=0} = -\frac{\varepsilon(1-\varepsilon)\alpha(1-\alpha)}{(\alpha+\varepsilon(1-\alpha))^3} - \frac{\alpha Z}{\alpha+\varepsilon(1-\alpha)}. \tag{12}$$

A useful consequence of formula (12) is that for $\varepsilon \ll \alpha$, regardless of the value of α, an approximate relationship holds:

$$\frac{d}{d\theta}\left(\frac{n_{\mathrm{EPR}}}{n_{\mathrm{ads}}}\right)_{\theta=0} \approx -Z. \tag{13}$$

It can also be shown that under this condition ($\varepsilon \ll \alpha$), and additionally $\alpha \geq \frac{1}{Z}$, the maximum of n_{EPR} is approximately located at $\theta_{\max} \approx \frac{1}{Z+1}$ (see $\frac{n_{\mathrm{EPR}}}{N}$ in Fig. 5). In the case of a small relative fraction of strong centers ($\alpha \ll 1$), the maximum of n_{EPR} is located at $\theta_{\max}$ of the order of α if $\varepsilon \ll 1$ (Fig. 6a), but it shifts to the region of higher θ when the strengths of the adsorption centers approach each other (Fig. 6b).

References

1. P.H. Kasai, R.J. Bishop Jr., in *Zeolite Chemistry and Catalysis*, ed. by J.A. Rabo (American Chemical Society, Washington DC, 1976), pp. 350–391
2. P.H. Kasai, R.J. Bishop, J. Am. Chem. Soc. **94**, 5560 (1972)
3. A. Gutsze, M. Plato, H.G. Karge, F. Witzel, J. Chem. Soc. Faraday Trans. **92**, 2495 (1996)
4. J.H. Lunsford, J. Chem. Phys. **46**, 4347 (1967)
5. B.M. Hoffman, N.J. Nelson, J. Chem. Phys. **50**, 2598 (1969)
6. C.L. Gardner, M.A. Weinberger, Can. J. Chem. **48**, 1317 (1970)
7. J.H. Lunsford, J. Phys. Chem. **74**, 1518 (1970)
8. P.H. Kasai, R.M. Gaura, J. Phys. Chem. **86**, 4257 (1982)
9. A. Pöppl, T. Rudolf, D. Michel, J. Am. Chem. Soc. **120**, 4879 (1998)
10. M. Niwa, T. Minami, Y. Murakami, Bull. Chem. Soc. Jpn. **49**, 565 (1976)
11. S. Furuyama, T. Morimoto, R. Hirasawa, J. Phys. Chem. **82**, 1027 (1978)
12. A. Adamski, G. Djéga-Mariadassou, Z. Sojka, Catal. Today **119**, 120 (2007)
13. J.W. Jermyn, T.J. Johnson, E.F. Vansant, J.H. Lunsford, J. Phys. Chem. **77**, 2964 (1973)
14. A.M. Volodin, K.A. Dubkov, A. Lund, Chem. Phys. Lett. **333**, 41 (2001)
15. P. Fisicaro, E. Giamello, G. Berlier, C. Lamberti, Res. Chem. Intermed. **29**, 805 (2003)
16. A. Volodin, D. Biglino, Y. Itagaki, M. Shiotani, A. Lund, Chem. Phys. Lett. **327**, 165 (2000)
17. V.A. Bolshov, A.M. Volodin, G.M. Zhidomirov, A.A. Shubin, A.F. Bedilo, J. Phys. Chem. **98**, 7551 (1994)
18. I. Langmuir, J. Am. Chem. Soc. **40**, 1361 (1918)
19. D. Graham, J. Phys. Chem. **57**, 665 (1953)
20. S. Brunauer, *The Adsorption of Gases and Vapors. Volume 1: Physical Adsorption* (Princeton University Press, Princeton, 1945)
21. J. Koresh, A. Soffer, J. Colloid Interface Sci. **92**, 517 (1983)
22. P.M. Mathias, R. Kumar, J.D. Moyer, J.M. Schork, S.R. Srinivasan, S.R. Auvil, O. Talu, Ind. Eng. Chem. Res. **35**, 2477 (1996)